FINITE ELEMENT ANALYSIS OF THE AXIAL COMPRESSION OF TUBES

A.A.N. Aljawi and M. H. M. Ahmed

Department of Production Engineering, College of Engineering,
King Abdulaziz University, P.O.Box 9027, Jeddah 21413
Kingdom of Saudi Arabia

ABSTRACT

The axial compression of metallic tubes with circular cross-sections is associated with complicated deformation patterns that comprise absorbing considerable energy in the plastic range. Therefore, these tubes can be efficiently used as energy absorbers in structures, and equipment. The objective of this paper is to present the results of the analysis of the nature of deformation, and the involved forces, stresses, strains and energy during axial compression of circular tubes under variable conditions, using FEM. A powerful and flexible FEM package (ABAQUS/Explicit, Version 5.73) has been applied to cover the large plastic deformation under a variety of strain rates (rate-dependent plasticity). The analysis is extended to include the effects of some prominent variables such as the speed of deformation, and tube thickness.

Keywords: Finite Element Analysis, Axial Compression, Metallic Tubes, Modes of Deformation, Energy

INTRODUCTION

The axial compression of metallic tubes with circular cross-sections provides an efficient mechanism for absorbing energy during collapse. This is due to the large plastic deformation that they can take, under specific conditions, in the form of successive axial folds which is known as the axi-symmetric mode of deformation or the "concertina" mode. Other modes of deformation include the "diamond" mode or non-axial symmetric (successive folds in both the axial and circumferencial directions), the mixed mode (concertina and diamond), and the Euler buckling mode which takes place at high slenderness ratios [1]. However, these modes absorb less energy during collapse, and accordingly, the conditions leading to any of them should be avoided when designing the tube as energy absorbent [2]. Other tube geometries such as the frusta (truncated conical shape), and square sections are also less efficient in absorbing energy during collapse [3-5]. The variables which tend to form the concertina mode of deformation are higher tube thickness, higher yield strength of the material, high friction at the tube-platen interface, controlled thickness/diameter ratio, and lower length/diameter ratio [2, 6].

Several attempts have been made towards theoretical analysis of the forces, stresses, and energy for the concertina deformation mechanism. These investigations were based on simplified equilibrium approach or energy balance approach, and neglected some aspects as friction, or redundant work, which usually led to force or stress values much lower than those experimentally measured [7-10]. The Finite Element Method (FEM), is a powerful tool for the analysis of complicated deformation problems. The technique has been used to study similar problems but not with large plastic strains, such as the deformation of polymer composite tube materials [11], and the case of pretorsioned pipe cluster [12]. However, it has not been

yet directly applied to the problem of concern due to the complexity of the deformation mechanism.

THE ABAQUS FEM PACKAGE

The Finite Element Method is a well established computational technique for solving intricate linear and nonlinear continuum problems. Literature and procedures for applying this technique on a variety of engineering problems are available in too many references [13-17]. Several FEM packages have been developed recently, the most powerful of which is the ABAQUS. It is a flexible tool for finite element modeling. The version used in these investigations is the ABAQUS/Explicit, Version 5.73. This program provides nonlinear, transient and dynamic analysis of solids and structures using explicit time integration. Its powerful contact capabilities, reliability, and computational efficiency on large models also make it highly effective for quasi-static applications involving discontinuous nonlinear behavior. The program requires a hardware of at least Pentuim II, 400 MHz (for speedy runs), 64 MB of RAM configurations, and Windows NT operating system, with a high resolution graphics card (1024x768 in 256 colors). Double speed CD-ROM drive, 600 MB minimum free space, 4.3 GB hard disk, and17 inch monitor are recommended.

PROBLEM SPECIFICATIONS AND BOUNDRY CONDITIONS

The analysis is based on modeling of the axial symmetric concertina mode of deformation, and accordingly, the axi-symmetric module of the ABAQUS-Explicit program has been chosen. Therefore only one side of the tube needs to be considered for mesh generation. The type of element selected for the analysis is 4-node bilinear axisymmetric continuum element suitable for large deformation plasticity (CAX4R). The elements at the interface with the machine platen were selected as 2-node linear rigid element for axisymmetric planar geometries (RAX2).

A mild steel tube material is considered with yield stress 320 MPa, and strain hardening rate 1157 MPa/unit strain (Classical metal plasticity model using standard Mises yield surface with associated plastic flow). The tube has an internal diameter of 60 mm, length of 120 mm, and a thickness of 1.5 mm. The tube is axially deformed at a speed 0.25 m/sec. A high coefficient of friction of 0.35 is assumed to insure development of the concertina mode of deformation. To investigate the effects of geometric parameters, some dimensions are varied as will be stated in relevant sections.

The number of elements on the axisymmetric tube section for achieving convergence of results is selected as 390 quadrilateral element, and will be presented through the results (130 element in the axial direction x 3 in the radial direction of the thickness).

RESULTS

Force-Displacement Diagram

A typical force-displacement relation as predicted by the ABAQUS for the axial compression of the tube by 66.7% reduction in height, is shown in Figure 1. The figure includes the experimental force-displacement relation obtained previously [18] for comparison. Almost full conformance can be observed for the peak forces and number of waves. However, displacements of the experimental results are shifted to the right relative to theoretical values. This could be attributed to the rigid-plastic model assumed by the program when large plastic strains are considered. Additional displacement may also be required practically to reach full contact between platens and the tube (fill in). The number of waves shown in the figure (9 waves) corresponds to the number of outward and inward folds formed along the tube circumference.

Deformation Energy

Figure 2 shows the total internal energy consumed in the collapse of the tube presented as solid line, and the energy consumed in the plastic deformation presented as dotted line. The limited difference between the two lines represents the energy lost in friction. From the figure, it is clear that the energy consumed in the process increases linearly with the axial

compressive displacement of the tube. A number of fine waves appears on the linear relation, matching the number of folds formed during displacement, which suggests that the energy consumed in the progression of each fold till the flattening position is relatively small. It could be also concluded from the figure that the deformation energy increases with the increase of the number of folds formed on the tube surface. It is worth perceiving that the total internal energy represents the area under the force-displacement relation presented in Figure 1.

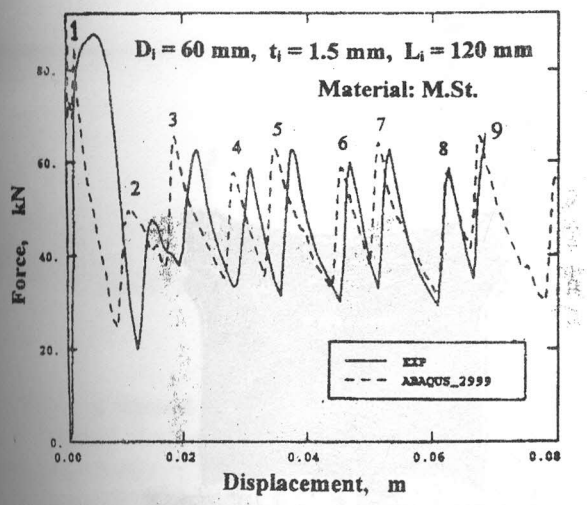

Figure 1 Computed and experimental force-displacement relation

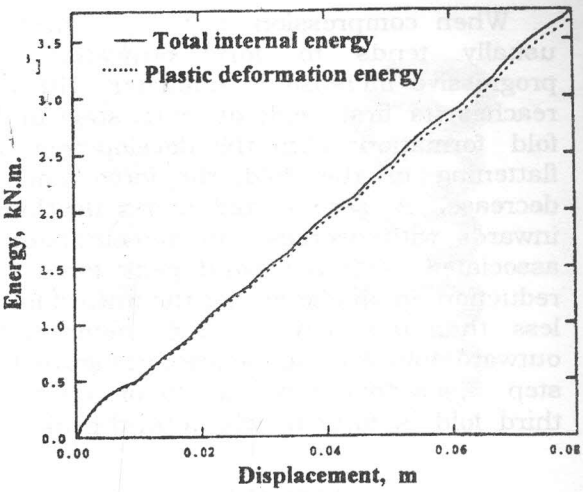

Figure 2 Energy-displacement relation

Mechanism of Deformation

Progressive deformation steps to form the concertina folds along the tube surface, at successively increasing displacements, are shown in Figure 3. These steps are selected at displacements matching the force peaks. The figure indicates that the number of folds formed outward are 5, and inward folds are 4, making a total of 9 folds (along a total displacement 65.3 % of the tube length). These folds correspond to the 9 waves on the force-displacement relation given in Figure 1.

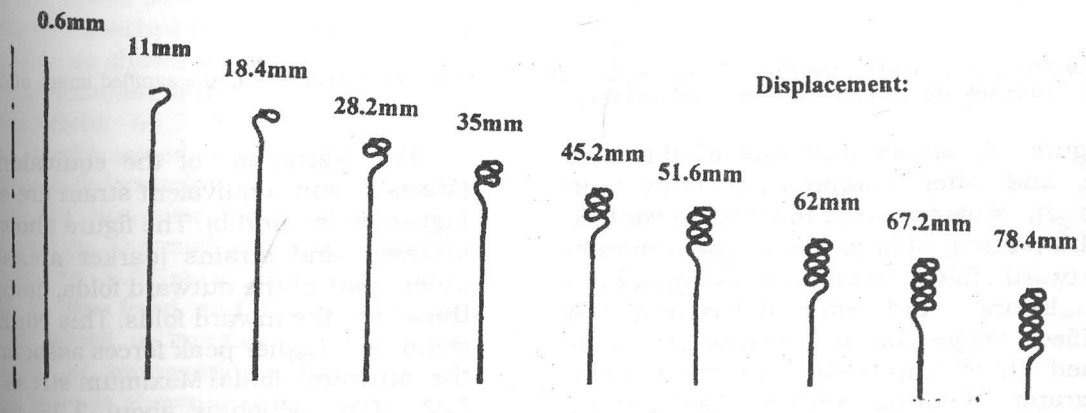

Figure 3 Steps of forming folds along the tube.

When compression starts, the first fold usually tends to form outwards, with progressive increase in diameter. The force reaches its first peak at early stage of this fold formation. With the development and flattening of the fold, the force tends to decrease. A second fold starts developing inwards with decrease in diameter (step 2), associated with a second peak force. The reduction in diameter for the inward fold is less than the increase in diameter in the outward fold as can be seen in Figure 4. At step 3, a second outward fold, or generally a third fold is formed with a third peak force (peak 3). This peak is larger than the second, due to larger lateral deformation in the outside direction as stated. The deformation continues progressing with inward folds 4, 6, and 8 associated with peak forces equal to the peak force of the second fold, and outward folds 5, 7, and 9 with peak forces equal to the peak of the third fold. Figure 1 ends with the tenth rise, indicative of the commence of the fifth internal fold at a final displacement 80 mm equivalent to a reduction in height 66.7 %.

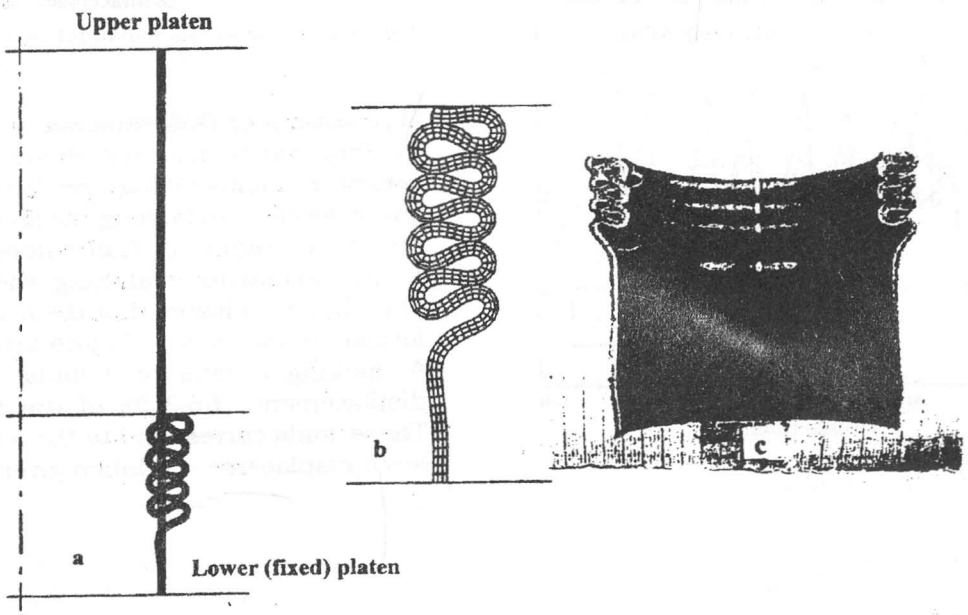

Figure 4 Mesh generated on the tube side before and after deformation (superimposed, a) magnified image of deformed tube side (b), and photo of deformed section (c)

Figure 4, shows one side of the tube before and after compression (step 9 in Figure 3), superimposed together to confirm the observation of larger lateral deformation on outward folds. The figure also shows the mesh before and after deformation. A magnified image of the deformed tube is attached (b) for improved observation, and a photograph (c) for half section of a deformed tube to confirm similarity of the analysis with experiments.

The variation of the equivalent stress (Mises) and equivalent strain are shown in Figure 5 (a and b). The figure shows higher stresses and strains (darker areas) at the inner part of the outward folds, compared to those at the inward folds. This confirms the trend of higher peak forces associated with the outward folds. Maximum stress value is 722 MPa which is about 2.25 times the initial yield stress of the material.

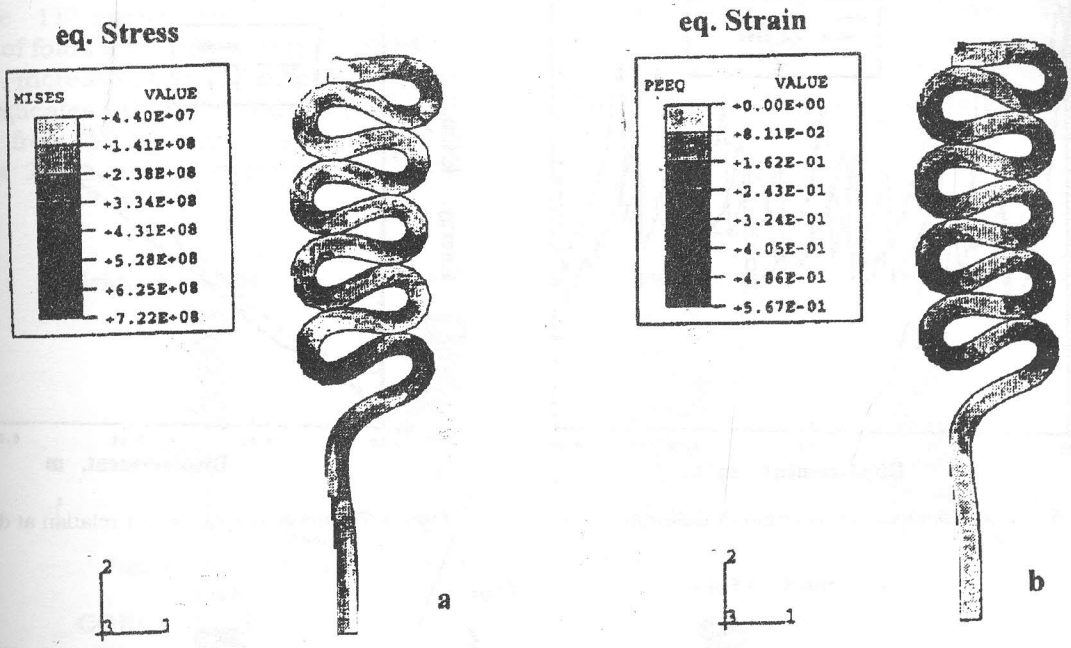

Figure 5 Distribution of Mises equivalent stress (a), and equivalent strain (b) along deformed tube section

Effect of Speed

Figure 6 shows the variation of the force-displacement relation for three axial compression speeds 0.5, 2, and 5 m/s. The figure indicates that the increase of the speed of deformation increases the peak forces, and shifts their position, i.e. changes the deformation sequence. The rise of the peaks with speed leads to an increase of the total energy absorbed by the material during deformation as shown in Figure 7. However, the energy increase is limited to only 8 % (at a displacement 66.7 %) with 10 times increase of the speed . The change of the sequence of deformation is shown in Figure 8, where the initiation and propagation of folds starts at the moving platen side when the speed is 0.5 m/s. The direction is reversed to the fixed end side of the press when the speed is increased to 2 m/s. A mixed case of propagation of fold formation on both sides is shown at a speed of 5 m/s. This can be correlated to the clear shift of the peak force positions and the non-consistency of the peak values at this speed as shown in Figure 6.

Effect of Tube Thickness

To study the effect of tube thickness, steel tubes of the same internal diameter and length but with thickness 1,2,3 & 4 mm have been investigated. Figure 9, shows the force-displacement diagram for these thickness values. The figure indicates clearly that as the thickness increases, the peak forces increase, and the resulting number of folds tends to decrease and their sequence is inclined to change. The rate of rise of the peak force is higher than the rate of surface area increase with thickness (with thickness increase from 1 to 4 mm, the area is increased 4.2 times whereas the peak force increased by about 6 times). Figure 10, shows that the total energy also increases with the increase of tube thickness, but at higher rate (the energy is increased 10.5 times with thickness increase 4 times).

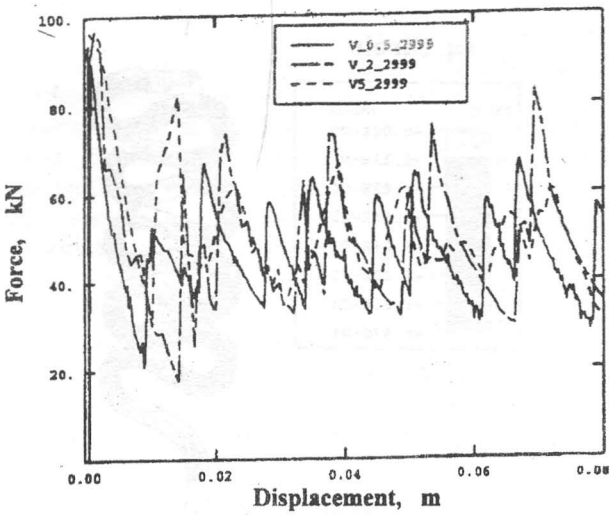

Figure 6 Force-displacement relation at different speeds

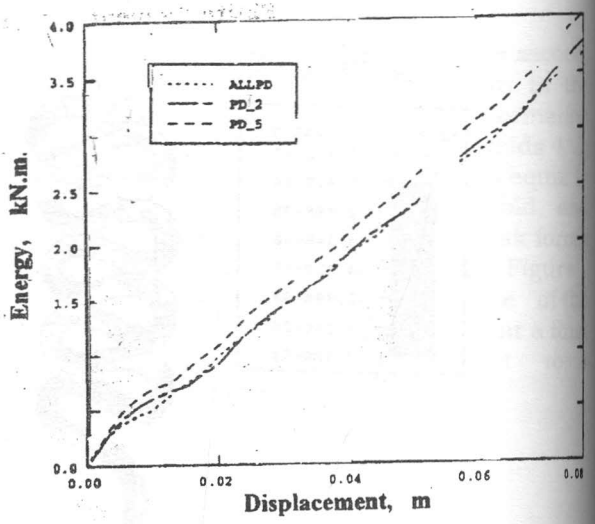

Figure 7 Energy-displacement relation at different speeds

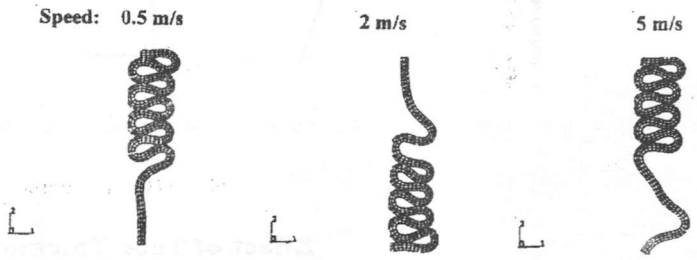

Figure 8 Effect of speed on the sequence of folds

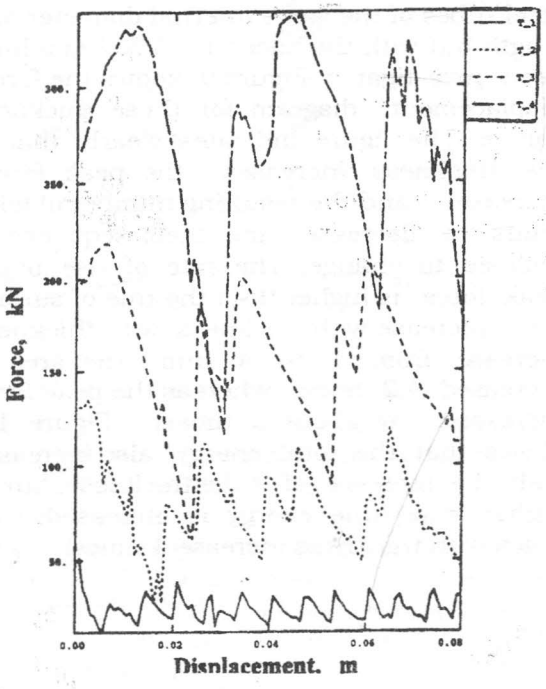

Figure 9 Force-displacement variation with tube thickness

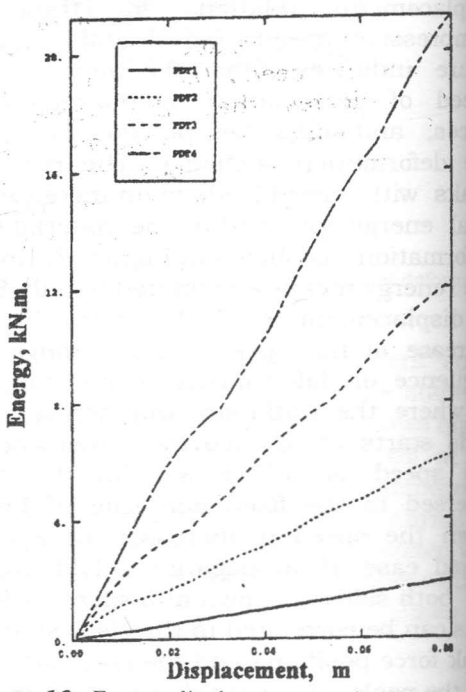

Figure 10 Energy-displacement variation with tube thickness

Figure 11 shows the change of the number of folds and their initiation direction with the increase of the tube thickness. The figure indicates that the number of folds decrease from 12 at thickness1 mm to 7 at thickness 2 mm, and further down to 5 folds at thickness 3 and 4 mm. The fold propagation changes from the moving platen side at lower thickness (1 and 2 mm) to the fixed end side as the thickness is increased (3 and 4 mm).

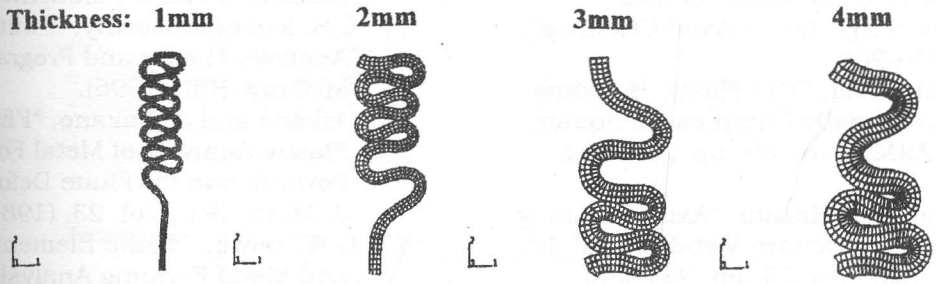

Figure 11 Effect of tube thickness on the number of folds and their sequence

CONCLUSIONS

- The Finite Element Analysis can fully represent the process of axial compression of tubes under conditions leading to axial symmetric concertina mode of deformation. Conformity with experimental results covers the load-displacement relation, deformation energy, and progression of concertina folds (mechanism of deformation).
- The load varies with displacement in wave form with a number of peaks equal to the number of folds.
- Folds change successively from outward to inward directions of the original diameter, with the outward folds consuming higher forces.
- Deformation energy increases linearly with the axial compressive displacement of the tube or with the number of folds.
- The increase of the compression speed increases the peak forces, the total energy absorbed by the material during deformation, and changes the deformation sequence from the moving platen side to the fixed end side of the press or to both sides.
- The increase of tube thickness leads to considerable increase of the peak forces, and the deformation energy. The resulting number of folds tends to decrease, and fold propagation changes from the moving platen side at lower thickness to the fixed end side as the thickness increases.
- The work presented in this paper is part of an extended research program to cover the effects of other variables, as well as three dimensional modes of deformation.

REFERENCES

1. L. Ervin Geiger, "Piping Handbook", Chapter A2, Syentek Books Company, Inc., (1991).
2. H.A. Youssef, M.H.M. Ahmed and A. Backar, "Experimental Study of the Axial Compression of Tubes", Under Publication in the MDP-7 Cairo, February 15-17 (2000).
3. W. Mamalis and Johnson, "The Quasi-Static Crumpling of Thin-Walled Circular Cylinders Under Axial Compression", Int. J. Mech. Sci., Vol. 25, pp. 713-732, (1983).
4. Mamalis, and W. Johnson, "Extensible Plastic Collapse of Thin-Wall Frusta as Energy Absorbers", Int. J. Mech. Sci., Vol. 26, pp. 537-547, (1984).
5. Macaulay, "Introduction to Impact Engineering", Chapmam and Hall Ltd., (1987).
6. Reid, "Plastic Deformation Mechanisms in Axially Compressed Metal Tubes Used as Impact Energy Absorbers", Int. J.

Mech. Sci., Vol. 35, pp. 1035-1052, (1993).
7. N.K. Gupta, R. Velmurugan, "Analysis of Axi-Symmetric Axial Collapse of Round Tubes", Thin-Walled Structures, Vol. 22, No. 4, pp. 261-274, (1995).
8. Yuichi Kitagawa and Masaaki Tsuda, "Dynamic Analysis of Thin-Walled Columns with Arbitrary Section Geometry Subjected to Axial Crushing", JSME, (1992).
9. Li and S.R. Reid, "The Plastic Buckling Analysis of Axially Compressed Square Tubes", ASME, Vol. 59, pp. 276-282, (1992).
10. Reddy and S. Al Hasani, "Axial Crushing of Wood-Filled Square Metal Tubes", Int. J. Mech. Sci., Vol. 35, pp. 231-246, (1993).
11. H. Hamada, S. Ramakrishna, "FEM for Prediction of Energy Absorption Capability of Crashworthy Polymer Composite Materials", J. of Reinforced Plastics and Composites, Vol. 16, No. 3, pp. 226-242, (1997).
12. K. Kormi, D.C. Webb, W. Jonson, "Application of the FEM to Determine the Response of a Pretorsioned Pipe Cluster to Static or Dynamic Axial Impact Loading", J. of Computers and Structures, Vol. 62, No. 2, pp. 353-368, (1997).
13. O.C. Zienkiewicz and R.L. Taylor, "The Finite Element Method", 2 Vols., McGraw-Hill, (1991).
14. J.N. Reddy, "Introduction to Finite Element Method", McGraw-Hill, (1993).
15. C.S. Krishnamoorthy, "Finite Element Analysis Theory and Programming", McGraw-Hill, (1996).
16. Oskada and J. Nakano, "FEM for Rigid-Plastic Analysis of Metal Forming Formulation for Finite Deformation", Int. J. Mech. Sci., Vol. 23, (1981).
17. G.W. Rowe, "Finite Element Plasticity and Metal Forming Analysis", Cambridge University Press, (1991).
18. T.M. Abu-Mansour and A.A.N. Aljawi, "Experimental Investigation of Axially Compressed Plastic Tubes as Impact Energy Absorbers", The 5th Saudi Engineering Conf., Vol. 4, pp. 57-68, March (1999).

Received August 17. 1999
Accepted September 2. 1999

تحليل العناصر المحدده للإنضغاط المحورى للأنابيب

عبد الغفار أزهرى الجاوى و محمود حامد أحمد
قسم هندسة الانتاج - جامعة الملك عبد العزيز

ملخص البحث

تصاحب عملية الإنضغاط المحورى للأنابيب ذات المقاطع المستديره بنماذج تشـــكل معقده تمتص قدر كبير من الطاقه فى المدى اللدن للتشـــكل، ولذلك فهذة الانابيب تستخدم بكفاءة عالية كأداه لإمتصاص طاقة الصدم في الإنشاءات و المعدات.

ويهدف هذا البحث الى تحليل طبيعة التشكل الناتج و دراسة القوى و الاجهادات و الانفعال و الطاقة الممتصة اثناء الانضغاط المحورى للانابيب الأسطوانيه تحت ظروف متباينه باستخدام نظرية العناصر المحدده ، وقد تم اســـتخدام حزمة برامج فعاله ومرنه لتطبيق النظريه هى (ABAQUS/Explicit, Version 5.7-3) لتغطية التشـــكل اللدن الكبير تحت تأثير معدلات انفعال متباينه (لدونه تتأثر بالتباين فى المعدل) ، كذلك تم تعميم التحليل ليشمل تأثير بعض المتغيرات كالسرعه، وسمك الأنبوبه.